Solidification of silicon in a one-dimensional slab and a two-dimensional wedge

Graham P. Benham[a], Kjetil Hildal[b], Colin P. Please[a], Robert A. Van Gorder[a*]

[a] *Mathematical Institute, University of Oxford, Andrew Wiles Building, Radcliffe Observatory Quarter, Woodstock Road, Oxford OX2 6GG United Kingdom*
[b] *Elkem Technology, Fiskaaveien 100, 4621 Kristiansand, Norway*
[*] *Robert.VanGorder@maths.ox.ac.uk*

Abstract

We have developed mathematical models in both one and two spatial dimensions for the solidification of silicon. The one-dimensional model describes slab casting related to a set of thin-casting experiments. The model is fitted to thermocouple data and accounts for various heat transfer mechanisms as well as the latent heat. The model can be used to predict the time taken for the material to completely solidify and the solidification distance (the point where solidification fronts meet which can be observed as a discontinuity in the grain microstructure). Simple approximate analytical results, which agree very well with the full-scale numerical solutions on Matlab and COMSOL, are provided. The two-dimensional model relates to a wedge casting experiment where, again, various heat transfer mechanisms and latent heat need to be accounted for. Experimental data from thermocouples is used to quantify the heat transfer coefficients by fitting to two-dimensional COMSOL simulations. A very simple analytical "Triangle model" is derived by assuming that the solidification fronts move as flat surfaces from each of the two wedge walls and the air surface, independently of each other, as three separate one-dimensional quasi-steady approximations. This model predicts that the area of liquid silicon will diminish as shrinking self-similar triangles. This simplified model provides analytical results for the solidification time and distances which agree very well with the COMSOL simulations.

Keywords: solidification of silicon, casting process, solidification fronts, Stefan problem

Nomenclature

c_{p_i}	$i = l,\ s$. The the specific heat capacity of liquid (l) and solid (s) silicon.
d	The depth of the silicon melt.
D	The solidification distance.
h_c	The conductive heat transfer coefficient.
h_a	The convective heat transfer coefficient.
k_i	$i = l,\ s$. The thermal diffusivity of liquid (l) and solid (s) silicon.
K	The ratio of solid to liquid thermal diffusivities.
κ	K multiplied by the ratio of solid to liquid specific heat capacities.
L	The latent heat of silicon.
$\mathbf{n}$	The outward facing unit normal to an interface.
N_c	The Nusselt number for conductive heat transfer to the mould.
N_a	The Nusselt number for convective heat transfer to the air.
N_r	The Nusselt number for radiative heat transfer to the air.
q_i	$i = l,\ s$ The heat flux in the liquid (l) and solid (s) silicon.
ρ	The density of silicon.
s_i	$i = 1,\ 2$. The positions of the solidification fronts.
σ	The Stefan-Boltzmann constant.
St	The Stefan number.
t^*	The solidification time.
T_m	The melting temperature of pure silicon.
T_0	The initial temperature of the liquid silicon before cooling.
T_∞	Room temperature.
T_{init}	The non-dimensional initial temperature of the silicon melt.
T_A	The non-dimensional room temperature.
θ	The enthalpy.
Θ	The non-dimensional enthalpy.
V_n	The speed of the solidification front in the normal direction.
ω	The position of the solidification front in two dimensions.
ϕ	The wedge angle coordinate.
α	The wedge angle.

1. Introduction

New markets demand high yield silicon of a more homogeneous consistency. It is well known that the cooling rates and mould size affect the microstructure and homogeneity of silicon during casting. The aim of this paper is to gain insight into the cooling rates that occur in two casting geometries. Typically, when cooling rates are too fast the silicon grains are very small (see Figure 1), causing dust, or 'fines', losses in the post-casting stage when the silicon is re-crushed. Although the yield is reduced, the small grains allow for a homogeneous distribution of impurities, which is an advantage in the silicon alloy

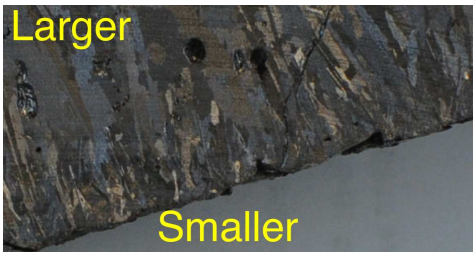

Figure 1: Fast solidification leads to small grains and a homogeneous distribution of impurities but large loss of yield due to wasted dust (fines) when material is re-crushed. Slow solidification leads to large grains and an inhomogeneous distribution of impurities, large-scale segregation in grain boundaries but high yield. We can see here that solidification occurred more quickly at the bottom edge of this sample due to the smaller grains. (Taken from experiment at Elkem on 04/06/15.)

industry. In contrast, when the silicon is cooled too slowly, the grains which form are much longer and hold impurities in the grain boundaries. These impurities are therefore distributed in a less homogeneous manner and, in fact, when the silicon is re-crushed, a large portion of them drop out from the long grain boundaries and are lost. For more specific details on the microstructure of silicon, see [1, 2].

Recent experiments have shown that the casting of silicon in small, thin containers shows promise for creating materials with good homogeneity. Hence the emerging interest in the silicon industry of the so-called 'thin-casting' technique. One dimensional solidification models are appropriate in thin casts where the aspect ratio is small. There has been extensive work on the mathematical modelling of these types of 'Stefan problems' where there is a solidification front which moves like the square root of time [3, 4, 5, 6, 7, 8, 9]. In these examples, similarity solutions only exist in the case of Dirichlet (constant temperature) or Neumann (no heat flux) boundary conditions and are therefore limited. In the case of small Stefan number, quasi-steady approximations can be made, rendering the problem considerably easier to solve [10, 11]. The existence of moving boundaries tend to make these problems difficult for numerical simulation yet many approaches have been examined [12, 13, 14, 15, 16]. This paper provides an analysis of the advantages and disadvantages of some of these analytical solutions for the purpose of direct comparison with silicon solidification experiments at Elkem and numerical simulations generated using COMSOL [17] and Matlab [18]. In particular, we find that the quasi-steady solution with linearised boundary conditions performs very well whilst providing simple analytical expressions for the temperature profile and position of the moving boundary. The application of the quasi-steady approximation to the domains and boundary conditions in this paper has not been explored in the literature. Furthermore, they are novel applications of mathematical modelling within the silicon manufacturing industry. The quasi steady solution, together with the parameter estimations given by the numerical simulations, will be useful for silicon manufacturers to predict the thermal history of the silicon and give approximate results for the solidification time and distance. The results will also apply to other solidification industries where the Stefan number is relatively small.

We will consider the case where the solidification of 100% pure silicon takes place due to cooling from both the metal mould and the surrounding air. The importance of different cooling mechanisms and cast depths will be investigated. We will use thermal data taken from these experiments to estimate the parameter values. The pure silicon case will give insight into the expected cooling rates that will be encountered even when impurities are present and is much simpler to analyse.

There has also been recent interest in casting in a wedge shaped mould to allow investigation of a range of cooling rates simultaneously. Perepezko and Hildal provide a comprehensive summary of the experimental work in this regard [19]. The problem of solidification in a wedge has been analysed mathematically and analytical solutions have been found in specific cases [20, 21, 22, 23, 24, 25]. But, as with the one dimensional problem, these analytical solutions are constrained to a limited selection of boundary conditions. We derive a simple 'Triangle model' using the 1D quasi-steady approximation from each edge of the wedge and from the air surface so that the solidification fronts emerge creating an region of liquid silicon which decreases in the shape of a self-similar triangle. This approximation, though crude, compares remarkably well with the full scale COMSOL simulation, whilst yielding simple analytical results. We use the COMSOL model to estimate the parameter values of the problem based on thermal data taken from Elkem experiments.

The paper is outlined as follows. In Section 2, we present the one dimensional model for the solidification of a silicon slab. We study the model through numerical simulations, while also obtaining analytical approximations to the solutions under relevant assumptions and reductions. We find that the aforementioned quasi-steady solution nicely captures the qualitative features of the numerical simulations. This permits us to better understand the solidification time for this silicon configuration. In Section 3, we consider the two-dimensional model of a silicon wedge. We run numerical simulations and obtain analytical approximations through a quasi-one-dimensional approach. The approximations agree quite well with the numerical simulations in the case where the wedge angle is small. Summarising comments and suggestions for future work are given in Section 4.

2. One Dimensional Model: Thin Casting

Heat flow in molten silicon above the melting temperature and in solid silicon below the melting temperature can be described by the heat diffusion equation with different coefficients in each region (see [26] for details). The phase transition for pure silicon is a sharp interface where the temperature is at the melting point and heat is released due to latent heat. We will assume pure silicon to allow us to use a sharp interface model but note that with impurities this interface would be diffuse which we shall not consider here.

Since the slab cast is wide, long and shallow the heat flow is dominated by flow through the depth and hence a one-dimensional model can be considered. The governing equation

for the temperature T is:

$$\rho_i c_{p_i} \frac{\partial T}{\partial t} = k_i \frac{\partial^2 T}{\partial x^2}, \tag{1}$$

where ρ_i, c_{p_i} , and k_i are the density, specific heat capacity and thermal conductivity of the liquid ($i = l$) and solid ($i = s$) respectively, which are all taken to be constant. Note that flow of the liquid has been neglected and the density change at the phase-boundary is quite small (about 2%) so the density will be taken constant ($\rho_l = \rho_s = \rho$).

The cast silicon is in the region $0 \le x \le d$ where $x = 0$ is the mould (made of copper) and $x = d$ is the surface interface with the air. Modelling including effects in the copper mould have been done but the results are similar to those found by assuming the copper is at constant temperature so we use this simplification from hereon. Contact between the silicon and copper results in conductive heat transfer while the air creates transfer by both radiation and convection. Boundary conditions for each of these surfaces can be modelled as follows:
at the copper/silicon boundary, $x = 0$,

$$k_s \frac{\partial T}{\partial x} = h_c \left(T - T_\infty\right) \tag{2}$$

at the silicon/air boundary, $x = d$,

$$-k_s \frac{\partial T}{\partial x} = h_a \left(T - T_\infty\right) + \sigma\epsilon\left(T^4 - T_\infty^4\right) \tag{3}$$

where T_∞ is the temperature (K) of the mould and the air, h_c is the conduction heat transfer coefficient ($WK^{-1}m^{-2}$), h_a is the convective heat transfer coefficient ($WK^{-1}m^{-2}$), σ is the Stefan-Boltzmann constant ($WK^{-4}m^{-2}$) and ϵ is the emissivity of silicon. Note that the radiative heat transfer is nonlinear and a common approximation, that allows simple analytical expression to be derived, is to linearise around the melting temperature T_m and to take

$$-k_s \frac{\partial T}{\partial x} \approx h_a \left(T - T_\infty\right) + \sigma\epsilon\left(\left(T_m^4 - T_\infty^4\right) + 4T_m^3 \left(T - T_m\right)\right) \tag{4}$$

There are two phase-boundaries and they emerge from each end of the liquid as it cools down to the melting temperature and overcomes the latent heat. Let the position of the phase-boundary near the mould be denoted $x = s_1(t)$ and that near the air by, $x = s_2(t)$ (see Figure 2). The temperature at these phase-boundaries is equal the melting temperature,

$$T(s_1(t), t) = T(s_2(t), t) = T_m. \tag{5}$$

and to change phase the latent heat, L ($J\ kg^{-1}$), of the silicon must be removed. Using conservation of heat gives the 'Stefan condition' at the phase-boundary that allows the heat flux to jump such that,

$$\rho L \frac{\mathrm{d}s_i}{\mathrm{d}t} = q_l - q_s, \quad i = 1, 2, \tag{6}$$

where $q = -k\frac{\partial T}{\partial x}$ is the heat flux in the x direction. We also impose the initial condition

$$T = T_0 \quad \text{when} \quad t = 0. \tag{7}$$

Constant	Typical Value	Units
T_m	1683	K
T_0	1700	K
T_∞	293	K
d	$0.03 - 0.1$	m
ρ	2533	$kg\ m^{-3}$
L	1798060	$J\ kg^{-1}$
k_l	43	$Wm^{-1}K^{-1}$
k_s	23.5	$Wm^{-1}K^{-1}$
c_{p_s}	970	$J\ kg^{-1}K^{-1}$
c_{p_l}	970	$J\ kg^{-1}K^{-1}$
σ	5.67×10^{-8}	$Wm^{-2}K^{-4}$

Table 1: List of dimensional parameter values. All values were supplied by Elkem.

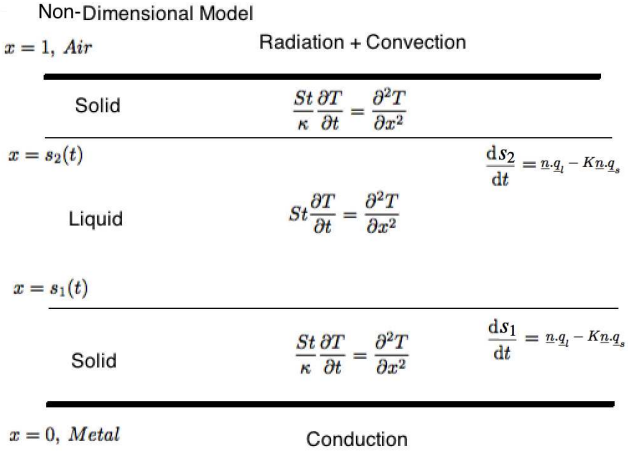

Figure 2: Diagram of the non-dimensionalised 1D model of the evolution of solid and liquid phases in the solidification of silicon.

A list of the well known values of the parameters can be found in Table 1. There are however three parameters that are not easily available and these are h_a, h_c and ϵ all related to the surface heat transfer rates. Although these can be estimated using empirical laws the approach taken here was to use these parameters to fit the observed experimental data.

2.1. Non-Dimensionalisation

Let us use the following scalings for each variable,

$$t = \frac{\rho L d^2}{k_l \left(T_m - T_\infty\right)} \hat{t}, \quad x = d\ \hat{x}, \quad T = T_m + \left(T_m - T_\infty\right) \hat{T}. \tag{8}$$

Then, our model becomes (dropping the hat notation from hereon),

$$\frac{St}{\kappa}\frac{\partial T}{\partial t} = \frac{\partial^2 T}{\partial x^2} \quad \text{on} \quad 0 < x < s_1(t), \tag{9}$$

$$St\frac{\partial T}{\partial t} = \frac{\partial^2 T}{\partial x^2} \quad \text{on} \quad s_1(t) < x < s_2(t), \tag{10}$$

$$\frac{St}{\kappa}\frac{\partial T}{\partial t} = \frac{\partial^2 T}{\partial x^2} \quad \text{on} \quad s_2(t) < x < 1, \tag{11}$$

while the boundary and initial conditions become

$$\frac{\partial T}{\partial x} = -N_a(1+T) - N_r\left((1+T_A+T)^4 - T_A^4\right) \quad \text{at} \quad x=1, \tag{12}$$

$$\frac{\partial T}{\partial x} = N_c(1+T) \quad \text{at} \quad x=0, \tag{13}$$

$$T = T_{init} \quad \text{when} \quad t=0, \tag{14}$$

and the Stefan condition at the phase-boundaries becomes

$$\frac{\mathrm{d}s_1}{\mathrm{d}t} = K\left.\frac{\partial T}{\partial x}\right|_{s_1^-} - \left.\frac{\partial T}{\partial x}\right|_{s_1^+}, \; T=0 \quad \text{at} \quad x=s_1(t), \tag{15}$$

$$\frac{\mathrm{d}s_2}{\mathrm{d}t} = K\left.\frac{\partial T}{\partial x}\right|_{s_2^+} - \left.\frac{\partial T}{\partial x}\right|_{s_2^-}, \; T=0 \quad \text{at} \quad x=s_2(t). \tag{16}$$

Here we have defined the non-dimensional constants

$$St = \frac{c_{p_l}(T_m - T_\infty)}{L}, \qquad \kappa = \frac{c_{p_l}k_s}{c_{p_s}k_l}, \qquad K = \frac{k_s}{k_l},$$
$$N_c = \frac{h_c d}{k_s}, \quad N_a = \frac{h_a d}{k_s}, \quad N_r = \frac{\sigma\epsilon d}{k_s}(T_m - T_\infty)^3, \tag{17}$$
$$T_{init} = \frac{T_0 - T_m}{T_m - T_\infty}, \qquad T_A = \frac{T_\infty}{(T_m - T_\infty)},$$

and all of the approximate parameter values are given in Table 2. Note that N_c, N_r and N_a are the Nusselt numbers for each specific heat transfer mechanism and here we choose their value to fit the model to the experimental data. For a visual representation of this 1D model, see Figure 2. The Stefan number, which for typical silicon casting conditions has a value $St \approx 0.75$, represents the ratio of the sensible heat to the latent heat. It should be noted that all non-dimensional constants are $O(1)$, except for the Nusselt numbers, $N_a \approx 0.01$ and $T_{init} \approx 0.01$ which are relatively small.

Constant	Typical Value
St	0.75
K	0.55
κ	0.55
T_{init}	0.01
T_A	0.21
N_c	1.02
N_a	0.03
N_r	0.26

Table 2: List of Non-Dimensional Parameter values.

2.2. Numerical Solution

The problem stated in Eqs. (9-16) was solved using simple finite differences with the problem formulated to use the enthalpy method in Matlab [18]. For any material, the temperature and the enthalpy, or heat content θ, are related in a unique continuous way, and for a pure material, such as silicon, this can take

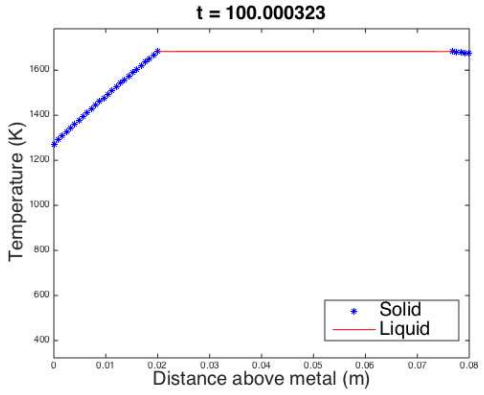

Figure 3: Numerical simulation of the two-phase Stefan problem (9-16) with conduction boundary conditions at $x = 0$ and radiation/convection boundary conditions at $x = d$. Here the depth of the cast is $d = 0.08$m. We can see the two solidification fronts emerging.

the non-dimensional form

$$T = \begin{cases} \frac{\kappa}{St}\Theta & \text{for} \quad \Theta < 0, \\ 0 & \text{for} \quad 0 < \Theta < \frac{1}{K}, \\ \frac{K}{St}\left(\Theta - \frac{1}{K}\right) & \text{for} \quad \frac{1}{K} < \Theta, \end{cases} \tag{18}$$

where $\Theta = \frac{k_l}{\rho L k_s}\theta - \frac{T_m c_s k_l}{L k_s}$. Now we can rewrite (11) in the much simpler form

$$\frac{\partial \Theta}{\partial t} = \frac{\partial^2 T}{\partial x^2}, \tag{19}$$

where Θ and T are related by (18). This relation accounts for the necessary jump in enthalpy as we cross from liquid to solid phase. An explicit timestepping method was used, although implicit methods are possible (see Voller et al. [14]). An example of the resulting temperature distribution is shown in Figure 3 and the time dependant behaviour has been fit to thermal data and shows suitable values for the heat transfer coefficients are $h_c = 300WK^{-1}m^{-2}$, $h_a = 10WK^{-1}m^{-2}$, and $\epsilon = 0.5$. This shows that the dominant heat transfer is to the mould, as indicated by the rapid motion of this phase-boundary, and the emissivity is reduced from the expected value due to surface effects. The same problem was also solved using the commercial package COMSOL [17] and these agreed closely with the Matlab calculations (see Figure 4 and Figure 5).

2.3. Analytical solutions

Some progress can be made in developing analytical solutions to the the problem stated in Eqs. (9-16) by considering special cases. One particularly helpful simplification, which is very realistic, is to consider the case where the molten silicon is just at the melting temperature, ($T_{init} = 0$) so that the temperature in the molten region is constant ($T = 0$) and the problem is then a one-phase Stefan problem. The movement of the two interfaces is then decoupled until they collide.

Much work has been done on finding similarity solutions to these types of problems where the solidification front moves

like $t^{1/2}$ (see [27] for examples). The special form of the similarity solutions requires that the boundary conditions are either fixed temperature or zero flux boundary conditions (see [6]). We have explored such solutions but these restrictions make these solutions not particularly useful in explaining the behaviour.

A second approach that is commonly taken is to consider small values of the Stefan number resulting in the quasi-steady approximation. Figure 3 indicates that the gradient of the heat in the solid region is approximately constant. This suggests that $\frac{\partial^2 T}{\partial x^2} \approx 0$, and therefore that we can ignore the time derivative in the heat equation. In fact $St \approx 0.75$ suggesting that this might not a particularly valid assumption, however it compares well with numerical simulations.

If we assume conduction/convection boundary conditions, the full problem near the bottom of the mould can be written as

$$\frac{\partial^2 T}{\partial x^2} = 0 \quad \text{on} \quad 0 < x < s_1(t), \tag{20}$$

$$\frac{\partial T}{\partial x} = N_c(1+T) \qquad \text{at} \quad x = 0, \tag{21}$$

$$T = 0 \qquad \text{at} \quad x = s_1(t), \tag{22}$$

$$s_1 = 0 \qquad \text{when} \quad t = 0. \tag{23}$$

The problem near the top surface can be posed in the same manner and the solution in the entire domain becomes

$$T(x,t) = \begin{cases} \frac{1+N_c x}{\sqrt{1+2KN_c^2 t}} - 1 & \text{on} \quad 0 < x < s_1(t), \\ 0 & \text{on} \quad s_1(t) < x < s_2(t), \\ \frac{(1+N_a - N_a x)}{\sqrt{1+2KN_a^2 t}} - 1 & \text{on} \quad s_2(t) < x < 1. \end{cases} \tag{24}$$

where the two moving boundaries are given by

$$\begin{aligned} s_1(t) &= \frac{1}{N_c}\left(-1 + \sqrt{1+2KN_c^2 t}\right), \\ s_2(t) &= \frac{1}{N_a}\left(1 + N_a - \sqrt{1+2KN_a^2 t}\right). \end{aligned} \tag{25}$$

Now we can find a closed form expression for the solidification time, t^*, at which the two boundaries collide $s_1(t^*) = s_2(t^*)$. This closed form expression is quite complicated and long but we can simplify it in the specific case where $N_a = N_c = N$ (when the problem is symmetric). Then we find that

$$t^* = \frac{1}{8KN}(4+N), \tag{26}$$

and, of course, the boundaries meet at $x = \frac{1}{2}$.

One important observation is that the solidification time for the quasi-steady solution varies with the cast depth d almost linearly (see Figure 4).

It should be noted that if we include any radiative terms in the boundary conditions, this prevents us from obtaining the analytical solution to the quasi-steady problem. However, we find that a decent approximation occurs if we use the linearised version in equation (4).

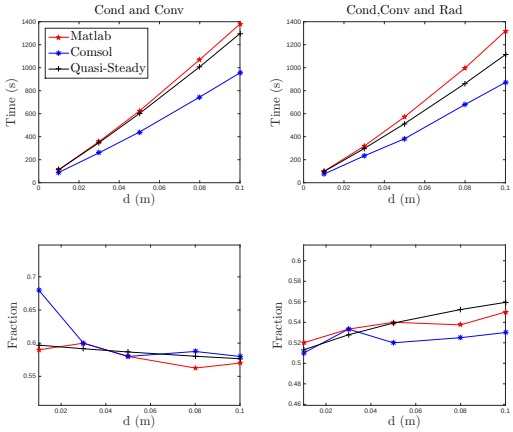

Figure 4: Comparison of dimensional solidification times, t^*, and nondimensional fractional solidification distance, D/d, predicted from numerical and analytical solutions for varying cast depth d. Each column contains different physics and therefore should not be compared directly. Only the solutions in each graph should be compared. The heat transfer coefficients used were $h_c = 180WK^{-1}m^{-2}$, $h_a = 120WK^{-1}m^{-2}$ (for the case without radiation), $h_a = 10WK^{-1}m^{-2}$, (with radiation) and $\epsilon = 0.5$. Numerical solutions were made on Matlab and COMSOL and the quasi-steady solution is described in Eqs. (20)-(23) with the linearised boundary condition for the radiation.

Changes in cast depth are not expected to affect the heat transfer coefficients significantly so, once we have fitted the coefficients for one depth, we will know their values in general. It is of great interest in industry to be able to predict the "solidification time" $t = t^*$ when the material becomes entirely solidified. Another important feature is the 'solidification distance', which is the point, $x = D$ where the two phase-boundaries met. This point can be observed under a microscope as a clear discontinuity in crystal size. One of the easiest things that operators can control is the cast depth d. Thus, having derived solutions using various different approximations, Figure 4 compares the predicted t^* (in dimensional units) and D/d (the fraction of the cast depth) for various d using different approximations.

It seems that in all cases, the quasi-steady solution performs very well as a predicative tool. One interesting observation is that it appears that the solidification distance as a fraction of the total depth does not seem to depend on the total depth. Furthermore, the solidification time appears to vary almost linearly with cast depth.

2.4. Thermal Data

Elkem has provided thermal measurement data from several experiments that has been used to validate and calibrate the various mathematical models.

Attempts were made to fit the model to the data using various parameters. In Figure 5 we see how by fitting the numerical solution to the data by eye, over a set of 3 parameters, we can match the curves up to an error of around 15%. We also attempted to fit the curves using numerical optimisation software but found that it was unwieldy.

Note the two discontinuities in the time derivative of T in Figure 5. The observed discontinuities in the simulation data are probably due to the discontinuous enthalpy function and the discontinuity in thermal conductivity from solid to liquid.

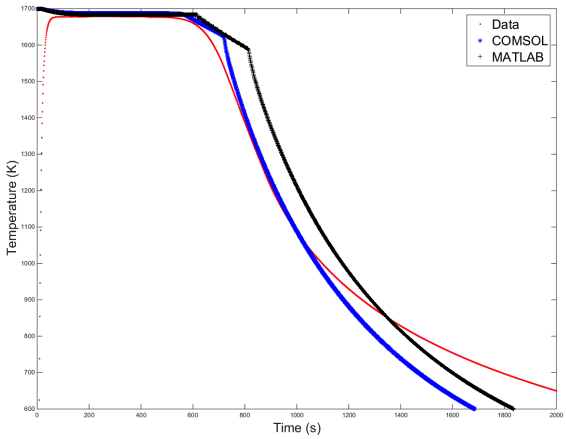

Figure 5: COMSOL and Matlab simulations of the thermal history of a point in the domain corresponding to thermocouple data from a casting experiment with $d = 0.08$m. Here we used all available parameters to fit (by eye) the predicitons to the data. The parameters used were the heat transfer coefficients $h_c = 300WK^{-1}m^{-2}$, $h_a = 10WK^{-1}m^{-2}$, and the emissivity of silicon $\epsilon = 0.5$.

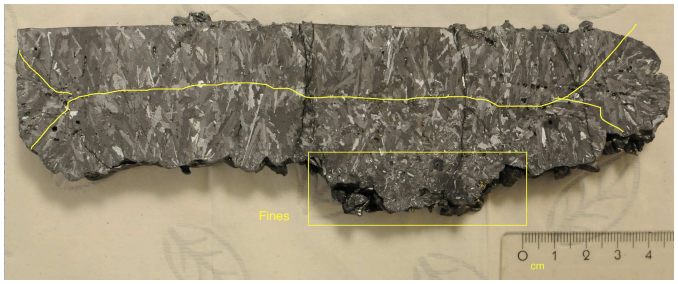

Figure 6: A cut section from a $3cm$ cast (with a $2cm$ layer of pre-laid fines) where we can see a discontinuity in the microstructure at approximately 50 – 60% depth. A yellow line has been drawn to indicate roughly where the two solidification fronts may have met. Solidification was slow enough at either side of the interface meeting point allowing larger grains to form.

Furthermore, even if there were some sharper changes in the temperature, the thermocouple would smooth them out a little due to its own internal heat diffusion. Since the aim of this paper is to provide simple insight in the general behaviour this discontinuities are not a major concern.

2.5. Grain Boundary Data

After the experiments the solidified casts were cut into sections to observe the internal grain microstructure. Figure 6 shows a clear discontinuity in the microstructure at the position highlighted by the yellow line which corresponds to the place where the two solidification fronts met.

Using the quasi-steady model given in Eqs. (20)-(23), we can derive an exact expression for the solidification distance, given the parameters of the problem. We can now formulate an inverse problem, where we know the solidification distance and want to derive the parameters. The solidification distance D, is found to be

$$\frac{D}{d} = \frac{N_c(2 + N_a)}{2(N_a + N_aN_c + N_c)}. \tag{27}$$

Therefore, given a solidification distance, D, and one of the Nusselt numbers, we can find the other Nusselt number explicitly, and therefore the corresponding heat transfer coefficient. We have not done any further grain boundary analysis, but it would be of interest to investigate how the predicted grain boundaries match up with those in reality.

3. Two Dimensional Model: Wedge Casting

The ideas outlined for analysing the one-dimensional slab problem can now be applied to consider heat flow in a wedge caster. The two dimensional Stefan problem is a simple extension of Eqs. (9-16). We can use the same dimensional scalings and non-dimensional constants, the only difference is the second order x derivative in Eqs. (9-11) is replaced by the Laplacian operator. For solid silicon, we have

$$\frac{St}{\kappa}\frac{\partial T}{\partial t} = \nabla^2 T, \tag{28}$$

while for liquid silicon, we have

$$St\frac{\partial T}{\partial t} = \nabla^2 T. \tag{29}$$

The Stefan condition (15-16) is altered to

$$V_n = K\underline{n} \cdot \underline{\nabla T}\big|_{solid} - \underline{n} \cdot \underline{\nabla T}\big|_{liquid}, \quad t = \omega(x, y), \tag{30}$$

where the phase-boundary is given by $\omega(x, y) = t$ and V_n is its speed in the normal direction $\underline{n}$ (see [3] for more details).

Elkem performed experiments to investigate casting silicon in a wedge-shaped mould. The company are interested in wedge casting because it allows for solidification over a large range of cooling rates in one run. Upon cutting the solidified cast, it is possible to pinpoint areas of desired microstructure, and when compared with a suitable model, we can extract the corresponding heat transfer coefficients. The wedge used in the experiment is of angle $\frac{\pi}{4}$, but wedge casters with larger or smaller wedge angles are of interest so we let the angle coordinate ϕ be such that $0 < \phi < \alpha$, where α is the wedge angle.

3.1. Numerical and analytical solutions

The two dimensional problem given in Eqs. (28), (29) and (30) with conduction to the graphite, and convection and radiation to the air was solved using COMSOL in a wedge geometry relevant to the experiments. In this simulation the mould (graphite) was again taken to be at constant temperature. In Figure 7 we can see a particular example of the calculated position of the phase-boundary at various times.

Analytical methods have been applied to the problem of solidification in a wedge by several others see [20, 21, 22, 23, 24]. However, as with the slab geometry difficulties arise in finding analytical solutions in the presence of boundary conditions other than Dirichlet or Neumann. Furthermore, these analytical solutions require that the wedge extends to infinity. Here we present a simple yet unexpectedly insightful 'Triangle model' which yields an analytical solution for the solidification problem with Robin boundary conditions (which correspond to Newton's law of cooling) in a wedge of finite size.

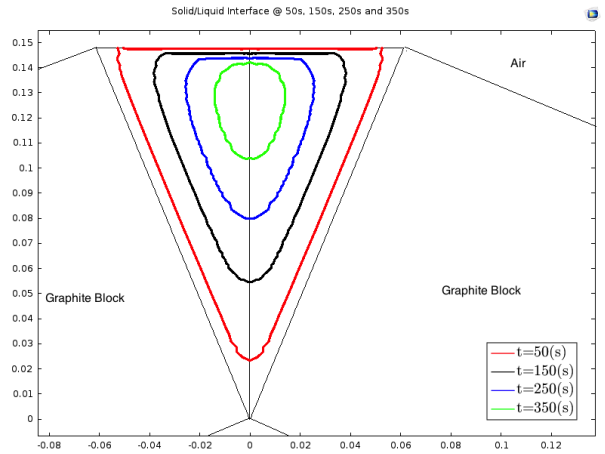

Figure 7: Solid/Liquid Interface position generated by the COMSOL model for a wedge of angle $\alpha = \frac{\pi}{4}$ at various times. The centreline represents a line of symmetry. Parameter values used in this model were $h_c = 850WK^{-1}m^{-2}$, $h_a = 10WK^{-1}m^{-2}$, $\epsilon = 0.5$.

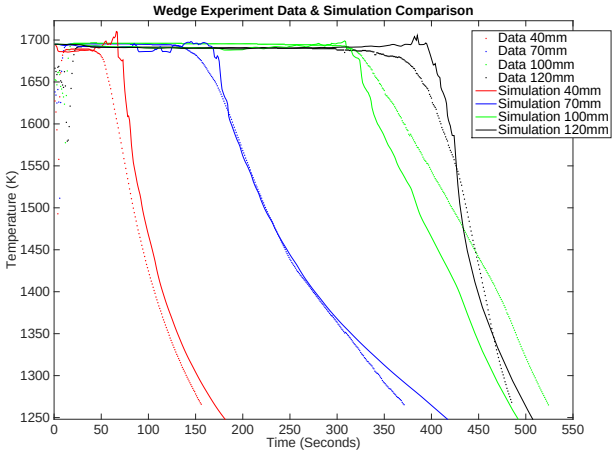

Figure 8: Wedge experiment temperature data compared with the temperature readings taken from corresponding points in the COMSOL model. As of yet the only fitting of parameters has been done by eye. The heat transfer coefficients used here were $h_c = 850WK^{-1}m^{-2}$, $h_a = 10WK^{-1}m^{-2}$ and $\epsilon = 0.5$.

The thermal history of the silicon was measured by four pyrometers at various heights and four pyrometers were also planted into the surrounding graphite blocks. The silicon pyrometer data, was used to determine the heat transfer coefficients by fitting the results of the COMSOL model, as shown in Figure 8. The approximate best parameter values from this fit are $h_c = 850WK^{-1}m^{-2}$, $h_a = 10WK^{-1}m^{-2}$, $\epsilon = 0.5$.

3.2. Triangle Model

Figure 9 shows a cross-sectional cut taken from the experiments. The relatively uniform direction of grain growth from each respective edge indicates that the solidification fronts move away parallel to the graphite and air surfaces and do not interact much. This suggests that perhaps a 1D model is appropriate at each boundary and we use the quasi-steady approximation for each of the three one dimensional problems. By symmetry we only need to consider the right-half of the wedge, and so take the solidification front from the air surface to be a straight line $y_1 = a_1 x + b_1(t)$ and the front from the graphite to

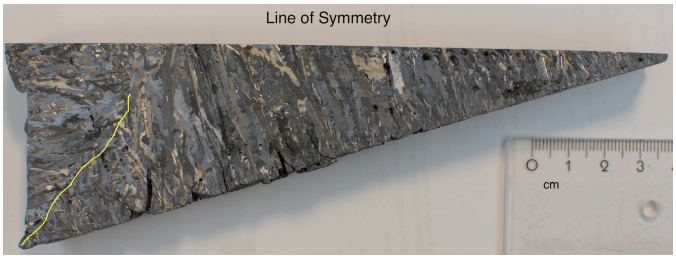

Figure 9: Cross-sectional cut of the solidified silicon (see Figure 7). We can see from decreased grain size that the solidification was much quicker at the edges in contact with graphite and air (bottom and left). In general, grain growth is in the same direction as the motion of the solidification front. Here we can see at least two predominant growth directions (from each exposed edge). A yellow line has been drawn to indicate roughly where the two solidification fronts may have met.

be the horizontal line $y_2 = b_2(t)$. Neglecting radiation to make the algebra easy we find that as a function of time

$$y_1 = \cot\frac{\alpha}{2}x + \csc\frac{\alpha}{2}s_1(t) = \cot\frac{\alpha}{2}x + \frac{1}{N_c}\csc\frac{\alpha}{2}\left(-1+\sqrt{1+2KN_c^2 t}\right),$$

$$y_2 = \frac{1}{N_a}\left(1+N_a-\sqrt{1+2KN_a^2 t}\right), \qquad (31)$$

where α is the wedge angle, and N_c and N_a are the conductive and convective Nusselt numbers. We can derive similar expressions for the case where we include radiation and linearise the boundary conditions in equation (4). In Figure 10 we see how these solidification fronts evolve over time. Note this solution can be derived as the outer solution of a small-angle approximation but where each angle must be thought of as being small. In Figure 11, which accounts for conduction, convection and radiation (linearised where necessary), we compare the predicted solidification times, t^*, and solidification position $(0, D/d)$ of the Triangle model with the COMSOL model, as we vary the wedge angle α. The two models compare very well and, in fact, as $\alpha \to 0$, the solidification times of the two models appear to converge and the solidification distances do not differ by more than about 5%.

4. Conclusions

We have developed mathematical models in both one and two dimensions for the solidification of silicon. The one-dimensional model relates to a set of thin-casting experiments. We were able to compare the models to the temperature measurements, thereby estimating the heat transfer coefficients. With a fitted model, it was possible to predict the time taken for the material to completely solidify and the place where the solidification fronts met. The solidification distance can be validated by casting samples, where it is possible to observe a discontinuity in the grain microstructure. Further work could include this validation as well as a quantitative analysis of the grain size, via the time-averaged cooling rates and a reference curve such as Forwald discusses [2].

One extremely useful approximation is the quasi-steady approximation, which is equivalent to the case of small Stefan number. This particular model provides analytical results for

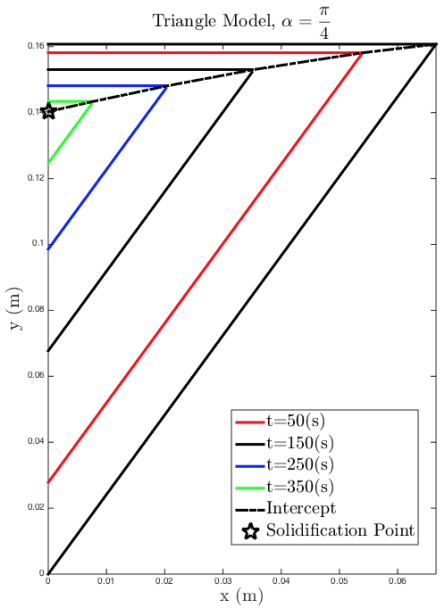

Figure 10: The solidification fronts predicted by the quasi-steady 'Triangle model' plotted at several times for wedge angle $\alpha = \frac{\pi}{4}$ and typical parameter values, $h_c = 850WK^{-1}m^{-2}$, $h_a = 10WK^{-1}m^{-2}$, $\epsilon = 0.5$. We have also marked the solidification point $(0m, 0.14m)$ at which the fronts met at $t = 417s$. We can compare the positions of these solidification fronts directly with those in the COMSOL simulation in Figure 7.

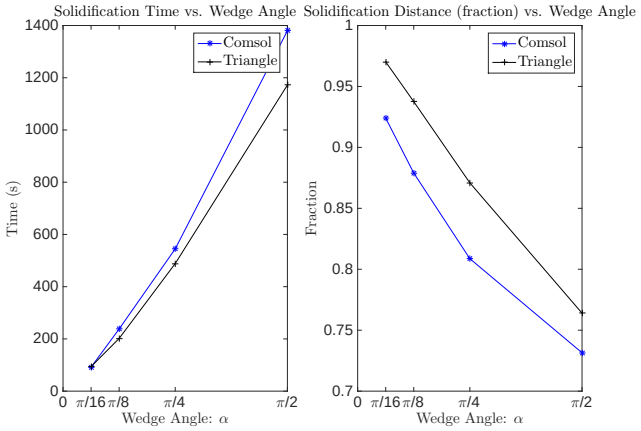

Figure 11: Comparison of the predictions of the solidification times (dimensional t^*) and solidification distance (nondimensional D/d) for both the COMSOL and the simplified Triangle model described in (31) with linearised radiation conditions. All the solidification fronts meet at $(0, D)$ where D is the solidification distance measured from the bottom tip of the wedge. We plot the fraction D/d where d is the depth of the bottom tip of the wedge.

the solidification time and distance which agree very well with the full-scale numerical solutions on Matlab and COMSOL.

The two-dimensional model relates to a wedge casting experiment. Using temperature measurements, we were able to estimate the heat transfer coefficients and thus obtained a good predictive numerical solution. If we assume that the solidification fronts move from each wedge wall independent of each other then we can use three separate one-dimensional quasi-steady approximations to create a 'Triangle model'. This predicts that the area of liquid silicon will diminish as shrinking self-similar triangles. This simplified model provides analytical results for the solidification time and distances which agree very well with the COMSOL simulation. The approximation becomes more accurate as we decrease the wedge angle α.

This initial investigation may now be extended to investigate impurities, their distribution, and the resulting impact on the silicon microstructure. The internal stresses and flow of the solidifying silicon could be explored as experimental observations show it expands, cracks and has significant gas movement as solidification progresses. We also add to the list of future work a more detailed analysis of the grain boundary data, with more accurate estimates for the solidification lines shown in Figures 6 and 9. Although the present results have been shown to agree well with experimental data, including these additional effects, would lead to a more accurate quantitative results.

Acknowledgments

This publication is based on work supported by the EPSRC Centre for Doctoral Training in Industrially Focused Mathematical Modelling (EP/L015803/1) in collaboration with Elkem. G.P. Benham thanks Elkem for financial support and the opportunity to work on-site during parts of this project.

References

[1] Schei, A., Tuset, J.K., and Tveit, H. 1998. Production of high silicon alloys. Tapir Trondheim, Norway.

[2] Forwald, K.R. 1997. Properties of some silicon rich alloys. NTNU Trondheim Metallurgisk Institutt 127, 147.

[3] Rubinstein, L. I., 1971. The Stefan Problem. 27 American Mathematical Society.

[4] Carslaw, H.S. and Jaeger, J.C. 1959. Conduction of heat in solids, 2nd edition. Clarendon Press, Oxford, UK.

[5] Crank, J. 1984. Free and moving boundary problems. Clarendon Press, Oxford, UK.

[6] Worster, M.G. 2000. Solidification of fluids. Perspectives in fluid dynamics 742, 393–446.

[7] Hill, J.M. 1987. One-dimensional Stefan problems: an introduction. Longman Sc & Tech.

[8] Visintin, Augusto. 2008. Introduction to Stefan-type problems. Handbook of differential equations: evolutionary equations 4, 377–484.

[9] Visintin, Augusto. 2012. Models of phase transitions. Springer Science & Business Media. 28.

[10] Louro, B. and Rodrigues, J.F. 1986. Remarks on the quasi-steady one phase Stefan problem. Proceedings of the Royal Society of Edinburgh: Section A Mathematics 102(3-4), 263-275.

[11] Barry, S.I. and Caunce, J. 2008. Exact and numerical solutions to a Stefan problem with two moving boundaries. Applied Mathematical Modelling 32(1), 83–98.

[12] Crowley, A.B. and Ockendon, J.R. 1979. On the numerical solution of an alloy solidification problem. International Journal of Heat and Mass Transfer 22(6), 941–947.

[13] Ockendon, J.R. and Hodgkins, W.R. 1975. Moving boundary problems in heat flow and diffusion. Clarendon Press, Oxford, UK.

[14] Voller, V., and Cross, M. 1981. Accurate solutions of moving boundary

problems using the enthalpy method. International Journal of Heat and Mass Transfer 24(3), 545–556.
[15] Le Bars, Michael and Worster, M Grae. 2006. Solidification of a binary alloy: Finite-element, single-domain simulation and new benchmark solutions. Journal of Computational Physics, 216(1), 247–263.
[16] Kutluay, S. 2005. Numerical schemes for one-dimensional Stefan-like problems with a forcing term. Applied mathematics and computation. 168(2), 1159–1168.
[17] Comsol, A.B. 2005. COMSOL multiphysics users guide. Version: September.
[18] MATLAB, Users' Guide and Statistics Toolbox Release. "Natick." MA: The Math Works (1990).
[19] Perepezko, J.H. and Hildal, K. 2006. Analysis of solidification microstructures during wedge-casting. Philosophical Magazine 86(24), 3681–3701.
[20] Hoang, H.V., Hill, J.M., and Dewynne, J.N. 1998. Pseudo-steady-state solutions for solidification in a wedge. IMA Journal of Applied Mathematics 60(2), 109–121.
[21] Rathjen, K.A. and Jiji, L.M. 1971. Heat conduction with melting or freezing in a corner. Journal of Heat Transfer 93, 101–109.
[22] Budhia, H. and Kreith, F. 1973. Heat transfer with melting or freezing in a wedge. International Journal of Heat and Mass Transfer 16(1), 195–211.
[23] Howarth, J.A. 1985. A note on two-dimensional linearized perturbations of the Neumann problem. International Journal of Heat and Mass Transfer 28(1) 301–304.
[24] King, J.R., Riley, D.S., and Wallman, A.M. 1999. Two–dimensional solidification in a corner. Proceedings of the Royal Society of London A: Mathematical, Physical and Engineering Sciences 455(1989), 3449–3470.
[25] Hoàng, Viêt Hà and Craster, RV. 2002. Wedge solidification with differing types of boundary conditions. IMA journal of applied mathematics. 67(6), 509–524.
[26] Crank, J. 1979. The Mathematics of Diffusion. Oxford University Press
[27] Howison, S.D. 1988. Similarity solutions to the Stefan problem and the binary alloy problem. IMA Journal of Applied Mathematics 40(3), 147–161.